New Control Strategy for Reducing Switching Losses in Three-Phase Voltage-Source PWM Converters*

Dong Xiaopeng, *IEEE Student Member*

Faculty of Electrical Engineering
Xi'an Jiaotong University
Xi'an, Shaanxi Province, China, 710049

Wang Zhaoan, *IEEE Senior Member*

Faculty of Electrical Engineering
Xi'an Jiaotong University
Xi'an, Shaanxi Province, China, 710049

ABSTRACT — In this paper, a new control strategy to reduce switching losses in three-phase voltage-source PWM converters is proposed according to Modified-Period-Average-Model (MPAM). The basic concept of this strategy is aimed at calculating the phase control voltages for controlling the source currents to be sinusoidal and in phase with the source voltages, and reducing the number of switching in each period.

The phase control voltages of Period-Average-Model(PAM) is obtained according to analyzing the operation of PWM converter. In order to reduce the sensitivity to system parameters in PAM, MPAM is deduced. Then a square wave whose frequency is three times of utility frequency is added to the phase control voltages derived from MPAM. The control strategy reduces the switching losses since there exists about one-third blanking time for every phase in one period. The theoretical derivation and the control strategy are experimentally verified on a 2.5 kW three-phase voltage source converter.

1. INTRODUCTION

VOLTAGE source PWM converters are the most popular in providing constant dc voltage and obtaining unity power factor with bidirectional power flow. Owing to these merits, they are frequently used in industrial application[1-3]. With the demands of clean power in recent years, the VSC is becoming increasingly attractive for its sinusoidal input currents. But the switching losses become a barrier when switching frequency is increased for better performance. To reduce the switching losses, one method is to use advanced semiconductor devices, another is to change the topology of converter by introducing the soft switching techniques[4-5], still another is to develop new control strategies.

In paper[6], various "dead-band" switching patterns are analyzed to increase the line-to-line amplitude voltage of inverters and reduce effective switching frequency in converter. In paper[7], one of the dead-band patterns is adopted to operate the VSC at increased utility voltage, which is complex in generating zero-sequence component.

In this paper, on the basis of analyzing the operation of VSC, the MPAM of three-phase voltage-source PWM converter and the phase control voltages in MPAM are obtained. Then a square wave whose frequency is three times of utility frequency is added to phase control voltages to reduce the effective switching frequency. At the end, the theoretical derivation and the control strategy are experimentally verified on a 2.5 kW three-phase voltage source converter. The control circuit is very simple and the control strategy keeps fine switching pattern and reduces the switching losses at least by 33%. The efficiency is improved and the sink is reduced.

2. MPAM FOR THREE PHASE PWM CONVERTER

* This project is supported by the National Natural Science Foundation of China

The circuit diagram of the three phase PWM converter is shown in Fig.1. Where k =a, b, c.

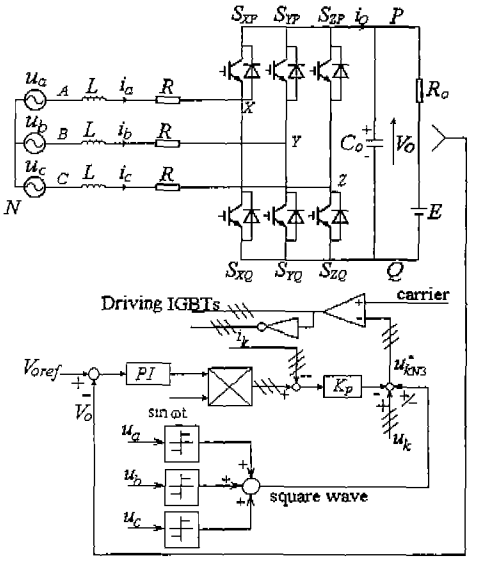

Fig.1 The three phase PWM converter

It is assumed that the source is balanced sinusoidal three phase voltage source with frequency ω. Taking the angle of the a-phase input voltage as the reference angle, three phase voltages are expressed as

$$\begin{aligned} u_a &= E_m \sin(\omega t) \\ u_b &= E_m \sin(\omega t - \frac{2\pi}{3}) \\ u_c &= E_m \sin(\omega t + \frac{2\pi}{3}) \end{aligned} \tag{1}$$

where E_m denotes the magnitude of the phase voltage.

From Fig.1, we get

$$u_{XN} = u_a - (Ri_a + L\frac{d}{dt}i_a) \tag{2}$$

where i_a is the a-phase source current. In order to achieve unity power factor, i_a must be sinusoidal and in phase with the a-phase source voltage u_a. From Equ.2, it can be seen that u_{XN} is the only control variable of i_a. By integrating both sides of the equation during the modulation period ($t = t_k$ to t_{k+1}) and dividing them by the modulation period T_{car}, We obtain

$$U^{\#}_{XNk} = U^{\#}_{ak} - (U^{\#}_{Lk} + U^{\#}_{Rk}) \tag{3}$$

where "#" denotes the period average value during T_{car}.

If the switching frequency is high enough, the $U^{\#}_{ak}$ can be replaced by u_a. Then Equ.3 can be written as

$$\begin{aligned} U^{\#}_{XN} &= u_a(t_k) - \frac{1}{T_{car}}\int_{t_k}^{t_{k+1}}\left(L\frac{d}{dt}i_a + Ri_a\right)dt \\ &= u_a(t_k) - \frac{L}{T_{car}}[i_a(t_{k+1}) - i_a(t_k)] - \frac{R}{T_{car}}\int_{t_k}^{t_{k+1}} i_a\,dt \end{aligned} \tag{4}$$

According to Equ.4, if the initial source current $i_a(t_k)$ and the final value $i_a(t_{k+1})$ in each modulation period are given, the average voltage of u_{XN} in the corresponding modulation period can be calculated under a condition of a constant modulation period T_{car}. It is assumed that the source current can obtain its desired final current $i_a^*(t_{k+1})$ in the end of the corresponding modulation period. That is $i_a(t_{k+1}) = i_a^*(t_{k+1})$. Then $U^{\#}_{XNk}$ can be expressed as its desired control voltage u^*_{XN}

$$u^*_{XN} = u_a - \frac{L}{T_{car}}[i_a^*(t_{k+1}) - i_a(t_k)] - \frac{R}{2}[i_a^*(t_{k+1}) + i_a(t_k)] \tag{5}$$

By substituting those instantaneous values or the initial values into corresponding values in Equ.5, we obtain the following control voltage

$$u^*_{XN} = u_a - \frac{L}{T_{car}}(i_a^* - i_a) - \frac{R}{2}(i_a^* + i_a) \tag{6}$$

Equ.6 is called as the PAM of PWM converter. But the model is still sensitive to system parameters L , R, and T_{car}. To minimize this sensitivity and take it into account that R is very small in practice, we get the MPAM of PWM converter by substituting $\frac{L}{T_{car}}(i_a^* - i_a) + \frac{R}{2}(i_a^* + i_a)$ with $k_p(i_a^* - i_a)$

$$u^*_{XN} = u_a - k_p(i_a^* - i_a) \tag{7}$$

where k_p is the gain.

Then we can get the single phase control block diagram of the proposed MPAM shown in Fig.2.

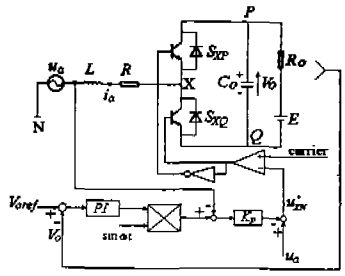

Fig.2 Single phase control diagram

3. ANALYSIS OF THE MPAM

The general model for PWM converter can be expressed as

$$\begin{cases} L\dfrac{di_a}{dt} + Ri_a = u_a - k_a v_o \\ L\dfrac{di_b}{dt} + Ri_b = u_b - k_b v_o \\ L\dfrac{di_c}{dt} + Ri_c = u_c - k_c v_o \\ C_o\dfrac{dv_o}{dt} = k_a i_a + k_b i_b + k_c i_c - \dfrac{v_o}{R_o} + \dfrac{E}{R_o} \end{cases} \tag{8}$$

where v_o is dc bus voltage; $k_n = S_n - \dfrac{S_a + S_b + S_c}{3}$ $\quad n = a,b,c$;

switching function S_n is defined as

$$S_n = \begin{cases} 1 & S_{nP} \quad ON \\ 0 & S_{nQ} \quad ON \end{cases}$$

When the switching frequency is high enough, the switching function S_n can be substituted by duty ratio d_n

$$d_n = \frac{1}{v_o}\left[u_n - k_p(i_n^* - i_n)\right] + \frac{1}{2} \tag{9}$$

By using d_n, the general model is written as

$$Z\dot{x} = Ax + Be \tag{10}$$

where

$$x = [i_a \;\; i_b \;\; i_c \;\; v_o]^T \tag{11}$$

$$e = [u_a \;\; u_b \;\; u_c \;\; E]^T$$

$$= [E_m \sin(\omega t) \;\; E_m \sin(\omega t - \frac{2\pi}{3}) \;\; E_m \sin(\omega t + \frac{2\pi}{3}) \;\; E]^T \tag{12a}$$

$$i^* = [i_a^* \;\; i_b^* \;\; i_c^*]$$

$$= [i_{cm} \sin(\omega t) \;\; i_{cm} \sin(\omega t - \frac{2\pi}{3}) \;\; i_{cm} \sin(\omega t + \frac{2\pi}{3})] \tag{12b}$$

$$A = \begin{bmatrix} -R & 0 & 0 & -(d_a - \frac{1}{3}\sum_{n=a,b,c} d_n) \\ 0 & -R & 0 & -(d_b - \frac{1}{3}\sum_{n=a,b,c} d_n) \\ 0 & 0 & -R & -(d_c - \frac{1}{3}\sum_{n=a,b,c} d_n) \\ d_a & d_b & d_c & -\frac{1}{R_o} \end{bmatrix} \tag{13}$$

$$Z = \begin{bmatrix} L & 0 & 0 & 0 \\ 0 & L & 0 & 0 \\ 0 & 0 & L & 0 \\ 0 & 0 & 0 & C_o \end{bmatrix} \tag{14}$$

$$B = \begin{bmatrix} 1 & 0 & 0 & 0 \\ 0 & 1 & 0 & 0 \\ 0 & 0 & 1 & 0 \\ 0 & 0 & 0 & 1/R_o \end{bmatrix} \tag{15}$$

where E_m denotes the magnitude of the phase voltage. i_{cm} denotes the magnitude of the reference current. "*" denotes reference values. The coefficient matrix A is time variant since d_n is a function of time. Fortunately, the duty ratio d_n is a sine function of time synchronized with the utility frequency. It is possible to transform the system to a rotating frame of reference in which it appears as time invariant[9]. The variables in ***abc*** stationary frame can be transformed into ***Fb*** rotating frame by applying the following transformation matrix T and its inverse matrix T^{-1}

$$T = \frac{1}{\sqrt{3}}\begin{bmatrix} 1 & e^{-j\omega t} & e^{j\omega t} & 0 \\ 1 & e^{-j(\omega t - \frac{2\pi}{3})} & e^{j(\omega t - \frac{2\pi}{3})} & 0 \\ 1 & e^{-j(\omega t + \frac{2\pi}{3})} & e^{j(\omega t + \frac{2\pi}{3})} & 0 \\ 0 & 0 & 0 & \sqrt{3} \end{bmatrix} \tag{16}$$

$$T^{-1} = \frac{1}{\sqrt{3}}\begin{bmatrix} 1 & 1 & 1 & 0 \\ e^{j\omega t} & e^{j(\omega t - \frac{2\pi}{3})} & e^{j(\omega t + \frac{2\pi}{3})} & 0 \\ e^{-j\omega t} & e^{-j(\omega t - \frac{2\pi}{3})} & e^{-j(\omega t + \frac{2\pi}{3})} & 0 \\ 0 & 0 & 0 & \sqrt{3} \end{bmatrix} \tag{17}$$

After transformation, the state variable vector x_r and voltage vector e_r in the rotating frame of reference become

$$x_r = \begin{bmatrix} i_0 \\ i_f \\ i_b \\ v_o \end{bmatrix} = T^{-1}x = \begin{bmatrix} 0 \\ \frac{1}{\sqrt{3}}\left[i_a e^{j\omega t} + i_b e^{j(\omega t - \frac{2\pi}{3})} + i_c e^{j(\omega t + \frac{2\pi}{3})}\right] \\ \frac{1}{\sqrt{3}}\left[i_a e^{-j\omega t} + i_b e^{-j(\omega t - \frac{2\pi}{3})} + i_c e^{-j(\omega t + \frac{2\pi}{3})}\right] \\ v_o \end{bmatrix} \tag{18}$$

$$e_r = \begin{bmatrix} e_0 \\ e_f \\ e_b \\ E \end{bmatrix} = T^{-1}e = \begin{bmatrix} 0 \\ \sqrt{3}E_m/2 \\ \sqrt{3}E_m/2 \\ E \end{bmatrix} \quad (19)$$

The differentiation of the state variable vector is

$$\dot{x} = T\dot{x}_r + \dot{T}x_r \quad (20)$$

Then, the state space equation of the converter (10) becomes

$$(T^{-1}ZT)\dot{x}_r = (T^{-1}AT - T^{-1}Z\dot{T})x_r + T^{-1}BTe_r \quad (21)$$

Substitution of (9) to (19)into (21) yields the state space equation in the rotating frame of reference

$$\begin{bmatrix} Li_0 \\ Li_f \\ Li_b \\ C_o\dot{v}_o \end{bmatrix} = \begin{bmatrix} -R & 0 & 0 & 0 \\ 0 & -R+j\omega L & 0 & a_{24} \\ 0 & 0 & -R_s - j\omega L & a_{34} \\ \sqrt{3}/2 & a_{42} & a_{43} & -1/R_o \end{bmatrix} \begin{bmatrix} i_0 \\ i_f \\ i_b \\ v_o \end{bmatrix} + \begin{bmatrix} 0 \\ \sqrt{3}E_m/2 \\ \sqrt{3}E_m/2 \\ E/R_o \end{bmatrix} \quad (22)$$

where

$$a_{24} = -a_{43} = -\frac{1}{v_o}\left[\frac{\sqrt{3}}{2}(E_m - k_p i_{cm}) + k_p i_f\right] \quad (23)$$

$$a_{34} = -a_{42} = -\frac{1}{v_o}\left[\frac{\sqrt{3}}{2}(E_m - k_p i_{cm}) + k_p i_b\right] \quad (24)$$

Because the zero sequence component $i_0 = 0$, this equation can be simplified to its reduced form:

$$\begin{bmatrix} Li_f \\ Li_b \\ C_o\dot{v}_o \end{bmatrix} = \begin{bmatrix} -R+j\omega L & 0 & a_{24} \\ 0 & -R-j\omega L & a_{34} \\ a_{42} & a_{43} & -1/R_o \end{bmatrix} \begin{bmatrix} i_f \\ i_b \\ v_o \end{bmatrix} + \begin{bmatrix} \sqrt{3}E_m/2 \\ \sqrt{3}E_m/2 \\ E/R_o \end{bmatrix} \quad (25)$$

4. DYNAMIC RESPONSE ANALYSIS

After transforming the converter model into the rotating reference frame, the converter represented by Equ.25 becomes a time-invariant system, but it is still a nonlinear one. Small signal linearization around its dc operating point can be applied for solution. Let

$$\left.\begin{bmatrix} i_f \\ i_b \\ v_o \end{bmatrix} = \begin{bmatrix} I_f \\ I_b \\ V_o \end{bmatrix} + \begin{bmatrix} \hat{i}_f \\ \hat{i}_b \\ \hat{v}_o \end{bmatrix} \right\} \quad (26)$$
$$i_{cm} = I_{cm} + \hat{i}_{cm}$$

By substituting these equations into Equ.25, omitting second-order terms, and separating the dc component from ac variation, both the steady-state dc model and the small signal ac model can be obtained. The steady state dc model is

$$0 = \begin{bmatrix} -R+j\omega L-k_p & 0 & 0 \\ 0 & -R-j\omega L-k_p & 0 \\ \frac{1}{V_o}[\frac{\sqrt{3}}{2}(E_m - k_p I_{cm}) + k_p I_b] & \frac{1}{V_o}[\frac{\sqrt{3}}{2}(E_m - k_p I_{cm}) + k_p I_f] & -\frac{1}{R_o} \end{bmatrix} \begin{bmatrix} I_f \\ I_b \\ V_o \end{bmatrix} + \begin{bmatrix} \frac{\sqrt{3}}{2}k_p I_{cm} \\ \frac{\sqrt{3}}{2}k_p I_{cm} \\ \frac{E}{R_o} \end{bmatrix} \quad (27)$$

Simplifying Equ.27, the steady state solutions can be obtained:

$$I_f = \frac{\sqrt{3}k_p I_{cm}}{2(k_p + R - j\omega L)}, \qquad I_b = \frac{\sqrt{3}k_p I_{cm}}{2(k_p + R + j\omega L)} \quad (28)$$

When only taking disturbance of i_{cm} into consideration, the small signal ac model can be expressed as

$$\begin{bmatrix} L\dot{\hat{i}}_f \\ L\dot{\hat{i}}_b \\ C_o\dot{\hat{v}}_o \end{bmatrix} = \begin{bmatrix} -R+j\omega L-k_p & 0 & -\frac{1}{V_o}(E_m-k_pI_{cm}+2k_pI_f) \\ 0 & -R-j\omega L-k_p & -\frac{1}{V_o}(E_m-k_pI_{cm}+2k_pI_b) \\ \frac{1}{V_o}[\frac{\sqrt{3}}{2}(E_m-k_pI_{cm})+2k_pI_b] & \frac{1}{V_o}[\frac{\sqrt{3}}{2}(E_m-k_pI_{cm})+2k_pI_f] & \frac{1}{V_o}[\frac{\sqrt{3}}{2}(E_m-k_pI_{cm})(I_f+I_b)+2k_pI_fI_b]-\frac{1}{R_o} \end{bmatrix} \begin{bmatrix} \hat{i}_f \\ \hat{i}_b \\ \hat{v}_o \end{bmatrix} + \begin{bmatrix} \frac{\sqrt{3}}{2}k_p \\ \frac{\sqrt{3}}{2}k_p \\ -\frac{\sqrt{3}}{2}k_p(I_b+I_f) \end{bmatrix} \hat{i}_{cm} \quad (29)$$

To analyze the dynamic response of peak line current $\hat{i}_m$, the transfer function between $\hat{i}_m$ and the control $\hat{i}_{cm}$ is required. Since $\hat{i}_m$ is not one of the variables in the rotating frame of reference, it is necessary to find the relations between the variables $\hat{i}_f$, $\hat{i}_b$, and $\hat{i}_{cm}$. It is known from the rotating transformation

$$i_m = \frac{2}{\sqrt{3}}\sqrt{i_f i_b} \quad (30)$$

Since

$$i_m = I_m + \hat{i}_m, \quad i_f = I_f + \hat{i}_f, \quad i_b = I_b + \hat{i}_b$$

and the first order approximation of Equ.30 about $i_f = I_f, i_b = I_b$ will be

$$\hat{i}_m = \frac{1}{\sqrt{3}}\left(\sqrt{\frac{I_b}{I_f}}\hat{i}_f + \sqrt{\frac{I_f}{I_b}}\hat{i}_b\right) \quad (31)$$

Applying Laplace transformation in Equ.29 and substituting variables in Equ.31, the transfer function between $\hat{i}_m$ and $\hat{i}_{cm}$ can be obtained

$$\frac{\hat{i}_m(s)}{\hat{i}_{cm}(s)} = \frac{k_p[(k_p+R)Ls+(k_p+R)^2+(\omega L)^2]}{\sqrt{(k_p+R)^2+(\omega L)^2}[L^2s^2+2(k_p+R)Ls+(k_p+R)^2+(\omega L)^2]} \quad (32)$$

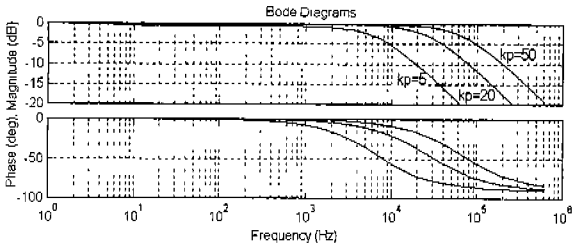

Fig.3 Frequency response of $\frac{\hat{i}_m(s)}{\hat{i}_{cm}(s)}$

The frequency response of $\hat{i}_m(s)/\hat{i}_{cm}$ is shown in Fig.3. From this transfer function and the steady state solution with $I_m \cong I_{cm}$, it is concluded that the peak line current i_m would follow the control i_{cm} with a nearly first order lag depending on the gain k_p. The higher k_p is, the higher the following speed.

5. IMPROVED CURRENT CONTROL STRATEGY WITH REDUCED SWITCHING LOSSES

It is known that the addition of zero-sequence components modifies the phase voltage but does not affect the line-to-line voltage. The following strategy can generate square wave u_3 whose frequency is three times of utility frequency simply as shown in Fig.1

$$u_3 = U_{car}[sign(u_a)+sign(u_b)+sign(u_c)] \quad (33)$$

Where U_{car} is the magnitude of the carrier wave form.

This square wave u_3 is used to generate a set of modified phase voltage commands u^*_{XN3}, u^*_{YN3}, and u^*_{ZN3}

$$\begin{cases} u^*_{XN3} = u^*_{XN} + u_3 = u_a - k_p(i^*_a - i_a) + u_3 \\ u^*_{YN3} = u^*_{YN} + u_3 = u_b - k_p(i^*_b - i_b) + u_3 \\ u^*_{ZN3} = u^*_{ZN} + u_3 = u_c - k_p(i^*_c - i_c) + u_3 \end{cases} \quad (34)$$

Similar results have been achieved by other algorithms[6,7] which are either based on angle information of the phase voltage or too complex to realize with analog circuit. The strategy implemented in this paper is different from the above mentioned algorithms in the following important ways.

1) Calculations for u_3 do not require any angle information about the phase voltage. This strategy is based only on the sign of the phase voltages.
2) It is very simple to obtain the square wave u_3. It is enough to implement with only three comparators and one amplifier.
3) In an open-loop control system for VSC, such as Phase-and-Amplitude control, the angle information is readily available and the phase control voltages are sinusoidal. For a closed-loop case as suboscillation current control, the phase control voltages commonly deviate from being perfect sinusoids. Since the u_3 in this strategy has nothing to do with the phase control voltages, it is very suitable to be used in such occasions.

One of the advantages of this control strategy is each of the phases does not switch for about one third of the cycle, which leads to great reduction in switching losses.

6. EXPERIMENTAL RESULTS

The system parameters for experimental verification were as follows:

utility phase voltage	88 Vrms
line inductor	4.7 mH
line resistance	0.2 Ω
dc bus voltage	250 V
load resistance	24 Ω
gain k_p	50

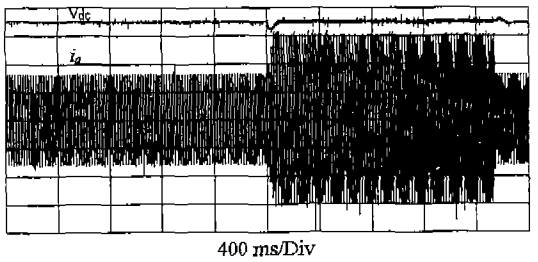

400 ms/Div

Fig.4 Experimental result when load changes i_a: 5.5A→10A→5.5A

Fig.4 and Fig.5 are the results when only employing the MPAM without adding the square wave. Fig.4 is the dc bus voltage and the a-phase current waveforms when the load changes. The phase current i_a varies from 5.5 A to 10 A and down to 5.5 A again. From the enlarged curve shown in Fig.5, it can be seen that the source current follows the load change quickly, which verifies the validity of the MPAM.

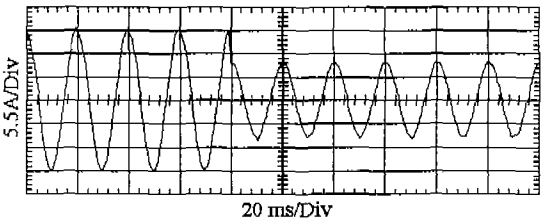

20 ms/Div

Fig.5 The enlarged result of fig.5

Fig.6 and Fig.7 are the experimental results when different square waves are added to the phase control voltages. The square wave in Fig.6 is in phase with the phase voltage while the square wave in Fig.7 is in reverse phase with the phase voltage. Fig.6(c) is the voltage on IGBT before adding the square wave. Fig.6(a) and Fig.7(c) are the voltages on IGBT after adding the square wave. It is obvious that the switching number of IGBT is reduced after adding the square wave.

Fig.6(b) and Fig.7(a) are the source current and its command current. It can be seen that when the square wave is in reverse phase with the phase voltage, the source current distortion is a little higher than that of when the square wave is in phase with the source voltage. But IGBTs do not switch around the peak of source currents in the former case, which reduces more switching losses than the latter. The phase control voltage is shown in Fig.7(c). Although each of the phases does not switch for about one third of the cycle, source currents are hardly affected negatively. Fig7.(d) is the harmonics analysis result of source currents which shows that the total harmonic distortion is still very low in spite of a little increase in 5 and 7 order harmonics. The

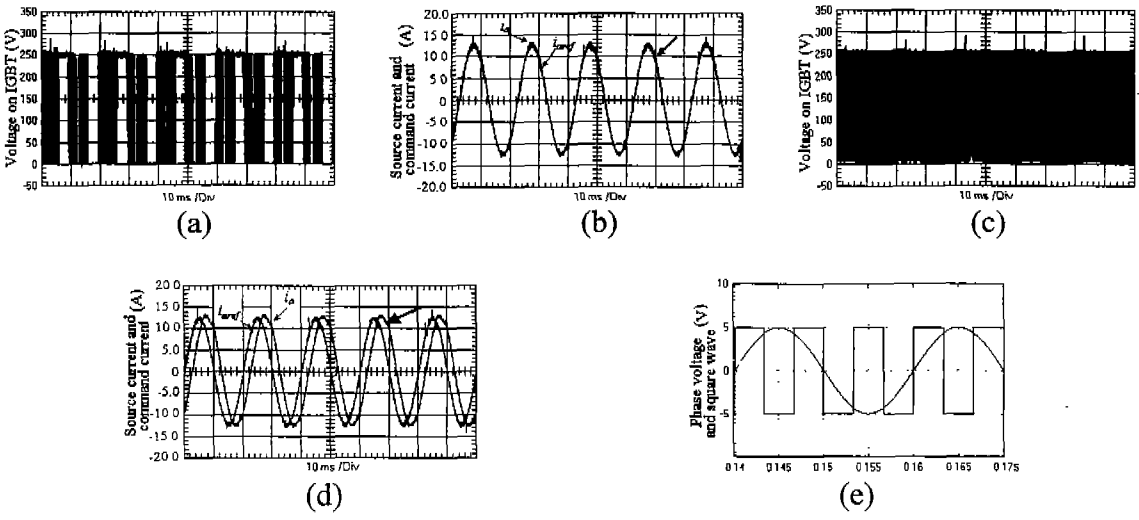

Fig.6 Experimental results after adding square wave in phase with source voltage
(a) voltage on IGBT after adding the square wave (b)the command current and a-phase current
(c) voltage on IGBT before adding square wave (d) the enlarged wave form of (b)
(e) the phase voltage and the square wave

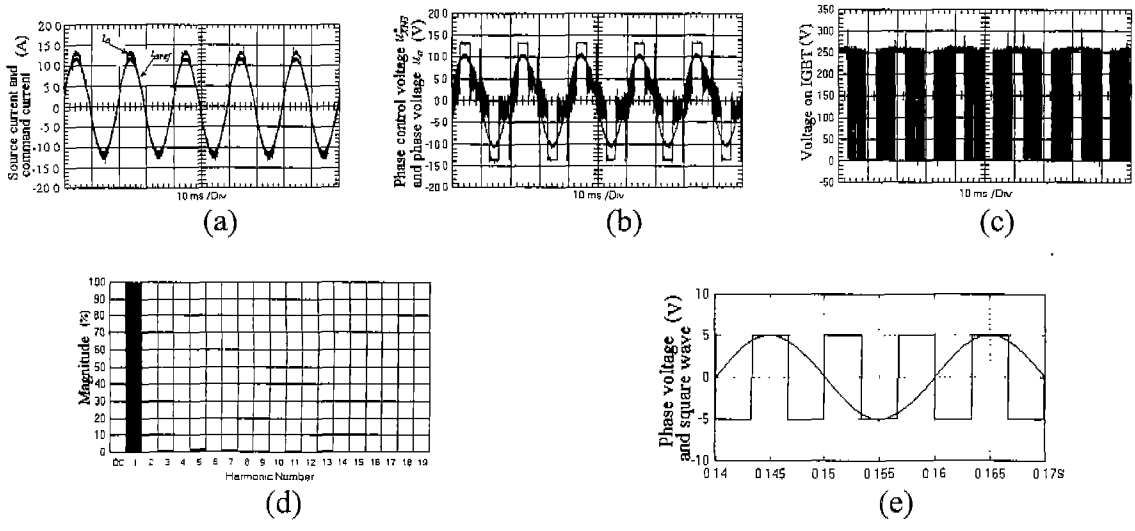

Fig.7 Experimental results after adding square wave in reverse phase with source voltage
(a) the command current and the a-phase current
(b) the source voltage u_a and the phase control voltage u^*_{XN3}
(c) voltage on IGBT after adding square wave (d) harmonics analysis result of source current
(e) the phase voltage and square wave

phase relations between phase voltage and square wave are clearly shown in Fig.6(e) and Fig7.(e).

7. CONCLUSION

According to the operation of PWM converter, the PAM is derived in this paper. But PAM is sensible to system parameters, which leads to the generation of MAPM to decrease the sensitivity. The phase control voltages are obtained simply in MAPM. It can be seen that the peak line current i_m in MAPM would follow the control i_{cm} with a nearly first order lag depending on the gain k_p. The higher k_p is, the higher the following speed.

A square wave is added to phase control voltages, which is capable to reduce switching losses in the VSC by at least 33% when the square wave is in reverse phase with phase voltage. If the square wave is in phase with phase voltage, experiments represent that the reduction of switching losses is not as much as that of the former. But the distortion of source current is better.

The method to generate square wave is simple and does not need any angle information of the phase control voltages, which makes the control strategy suit to close-loop application, such as suboscillation current control in which the phase control voltages commonly deviate from being perfect sinusoids.

REFERENCES

[1] J. W. Choi, S. K. Sul. "New current control concept – minimum time current control in the three-phase PWM converter." *IEEE Trans. Power Electron.*, Vol.12, pp. 124-131, 1997

[2] J. W. Dixon, B. T. Ooi. "Indirect current control of a unity power factor sinusoidal boost type 3 phase rectifier." *IEEE Trans. Ind. Electron.*, Vol.35, pp. 508-515, Jul., 1988

[3] A. Draou, Y. Sato, T. Kataoka. "A new state feedback based transient control of PWM AC to DC voltage type converters." *IEEE Trans. Power Electron.*, Vol.10, pp. 716-724, Nov., 1995

[4] Hua Guichao, Lee Fred C.. "Evaluation of switched-mode power conversion technologies." IPEMC'94, pp. 12-26.

[5] EH Ismail, R Erickson. "A new class of low-cost three-phase high-quality rectifiers with zero-voltage switching." *IEEE Trans. Power Elec.*, Vol.12, pp.734-742, Jul. 1997

[6] V. G. Agelidis, P. D. Ziogas, and G. Joos. ""Dead-band" PWM switching patterns." *IEEE Trans. Power Electron.*, Vol.11, No.4, pp.524-531, 1996.

[7] V. Kaura, V. Blasko. "Operation of a voltage source converter at increased utility voltage." *IEEE Trans. Power Electron.*, Vol.12, No.1,pp.132-137, 1997.

[8] Y. Nishida, M. Nakaoka, "Simplified predictive instantaneous current control for single-phase and three-phase voltage-fed PFC converters." *IEE Proc. - Electr. Power Appl.* , Vol.144, No.1, 46-52, 1997

[9] R. Wu, S. B. Dewan, G. R. Slemon. "Analysis of an AC to DC voltage source converter using PWM with phase and amplitude control." *IEEE Trans. Ind. Applicat.*, Vol.27, No.2, pp.355-364, 1991